International Journal of Electrical and Computer Engineering (IJECE)
Vol. 14, No. 4, August 2024, pp. 3592~3606
ISSN: 2088-8708, DOI: 10.11591/ijece.v14i4.pp3592-3606

Comparison performance study of singly-fed and doubly-fed induction generators-based bond-graph wind turbines model

Sugiarto Kadiman, Oni Yuliani
Department of Electrical Engineering, Faculty of Engineering and Planning, Institut Teknologi Nasional Yogyakarta, Sleman, Indonesia

Article Info

Article history:

Received Oct 29, 2023
Revised Mar 29, 2024
Accepted Apr 16, 2024

Keywords:

20-Sim software
Bond-graph
Doubly-fed induction generator
Law of mass conservation
Singly-fed induction generator

ABSTRACT

This paper consecrates to a comparative performance study of singly-fed and doubly-fed of induction generators thrusted by wind power turbine of similar generation capacity of 2.5 kW, and constant or variably wind speed. The singly-fed induction generator model could be represented using natural reference frame and doubly-fed induction generator model is described using a Park reference frame. Because of several physical domains existing in both induction generators like mechanical and electrical, modeling of generators is difficult, therefore the modeling based on physical methods takes a high credibility under these conditions. Among the procedures is Bond-graph method that models the systems based on law of mass conservation and/or law of energy conservation containing in the systems. Modeling the parts of both singly-fed and double-fed induction generators are based on Bond-graph method. We found that the impact of stator coil winding for on the current is in the form of changes of its value and steady state intervals; increasing the number of stator coil windings may also lead to increased stator current and the longer their steady state interval. Our study demonstrates also that doubly-fed induction generator possesses advantages compared to singly-fed induction generator, namely better current quality output and an adaptation to fluctuating wind speeds. The performance study is done in constant and variably wind speeds using simulated results of 20-Sim software.

Corresponding Author:

Sugiarto Kadiman
Department of Electrical Engineering, Institut Teknologi Nasional Yogyakarta
Babarsari, Catur Tunggal, Sleman, Yogyakarta, Indonesia
Email: sugiarto.kadiman@itny.ac.id

1. INTRODUCTION

Clean energy resources have turn out to be one of the most fascinating substitutes to reducing the consequences of climate change and its impact. One of main advantages is that they do not emit carbon dioxide or contaminate the air when they are used to produce electricity. Among all clean energy generation, wind energy has the quickest and most pertinent evolution of non-hydro renewable technology, not only from large scale wind farms but also from the growing penetration of stand-alone wind energy systems [1]–[4].

Stand-alone wind turbines offer an attracting clean energy resource for isolated areas or integrated rural. Wind turbines help in lowering the stress on the grid, reduce the pollution [5], and aside from fuel cost by decreasing diesel generators requirements which burn up heavy polluting fuel and may need added substantial costs for fuel transportation [6]. A stand-alone wind turbine can be allocated where great-quality wind resources are frequently placed and there is no get into to the grid [7].

However, to collide with fast development of power generation, recent researches in wind turbines are discussing concept of utilizing induction generator in standalone and small wind power system as a result of their superiorities more than synchronous generators, namely smaller dimensions, lesser charge, and minimal maintenance [8], [9]. Direct power conversion procedure utilizing singly-fed induction generator, such as squirrel cage induction generator, is extensively known in constant wind speed usages with reduced efficiency at higher speeds. Controlling a power flow needs a peripheral compensator of reactive power in order to regulate spreading of electrical line voltage and to avoid the entire system out of overload [10]. Conversely, a doubly fed induction generator with adjustable-speed capacity possesses greater energy efficiency, better power quality, and look like deceives concerned frequent attentions [11].

Induction generators, namely singly-fed and doubly-fed induction generators, are different domains and complex system that numerous methodological areas are built on, for example mechanical and electrical. Though, applying dissimilar procedures prior recognized and complicatedness of induction generators make achievable to visualize even dissimilar methodologies for their review and analysis. Because of its self-complexity, possibly having to use a general method for modeling the induction generator. Under these conditions, considering to analyze systems in a similar frame of reference, Bond-graph method is able to define complete configuration [12]–[14]. This technique has some properties are able to be performed to the model.

The Bond-graph structure comprises elements connected simultaneously through power bonds. The rapid power is substituted at *ports*. The allocating parameters by similar during in relation to operation among many *ports* as power parameters interpret like a function of time. Dissimilar variables of power are justified within a common structure known as *effort* and *flow*. The succession between *ports* that is *P= effort*flow* said to be instant power. Foremost advantages of Bond-graph method to simplify tools are unified graphical language way. They can define through physical observation of power interactions, energies segregation and storing occurrences in dynamic schemes concerning every physical domain. They visualize instruments of causality possessions for inscribing equivalences conforming to designated modeling premises.

Our study demonstrates that Bond-graph structure of doubly-fed induction generator owns advantages in comparation with Bond-graph structure of singly-fed induction generator, such as better current quality output and ability to regulate voltage caused by wind speed shifted. Outline of this study is as follows: first, the doubly-fed and singly-fed induction generator are evolved. Then, the complete models are simulated on 20-Sim package. Next part explains conclusion and evaluation. finally, closing stage of the study is described.

2. METHOD

A distinctive arrangement of a wind power is pointed in Figure 1. Variable speed wind turbines are able to receive highest energy convey utility over a widespread range of wind speeds. Wind turbine can continually adjust its rotational speed conversing into wind speed. This structure is constructed on an induction generator regarding a drive train and structural dynamics, such as blades, gearbox, and tower.

The flow of power in wind turbine is interpretation to bonds way. Huge torque is shaped by blades, then moves into gearbox over a main shaft. Gearbox converts large amount of torque into small one that adopted through generator. An equal circumstance is permissible for angular velocity, namely a fast-moving available aim at generator, altering by a gearbox into lower speed and accessible in turbine or hub.

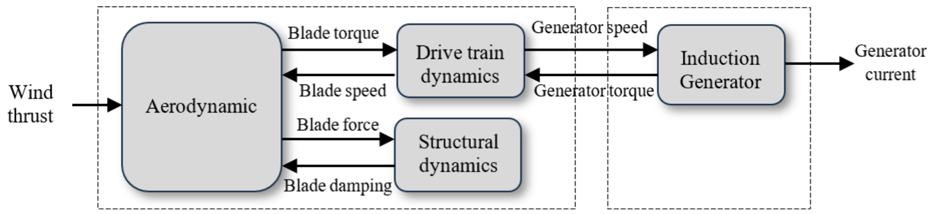

Figure 1. Sketch of wind turbine

2.1. Structure of wind turbine

Figure 2 displays a drawing of a wind power turbine [15], [16]. It involves of six of inertia bodies containing three of wind blades, hub or pivot, gearbox or housing of gear, and asynchronous or induction generator. Speed of wind and electromagnetic rotating force are the input variables. To obtain a dynamic equation for wind turbine based on the second of Newton principle could be somewhat problematical; some mistakes possibly will simply made. As a result, differential equations are obtained for a simplified instance.

Figure 3 shows a three-mass diagram of wind turbine. The drawing involves of hub, gearbox, and generator. Aerodynamic drag and electromagnetic rotating force are the inputs. All of variables are described in Table 1.

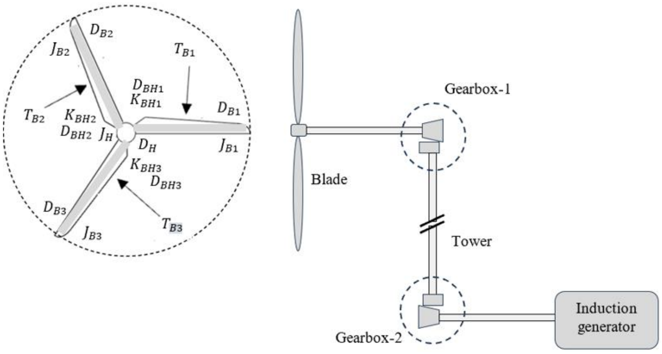

Figure 2. Generator connected blade via gearbox

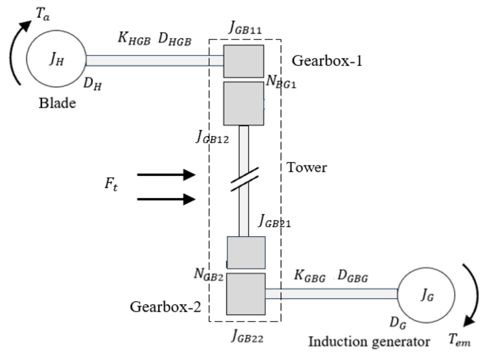

Figure 3. Shortened wind turbine structure

Table 1. Variables considering wind turbine structure

Abbrev.	Information	Abbrev.	Information
T_{B1}	Blade torque 1 as of wind	K_{HGB}	Stiffness among hub and gearbox
T_{B2}	Blade torque 2 as of wind	K_{GBG}	Stiffness among gearbox and generator
T_{B3}	Blade torque 3 as of wind	D_{HGB}	Damping among hub and gearbox
J_H	Hub inertia	D_{GBG}	Damping between gearbox and generator
D_H	Hub damping	J_G	Generator inertia
J_{GB11}	Gearbox 11 damping	T_{em}	Electromagnetic torque
J_{GB12}	Gearbox 12 damping	T_a	Aerodynamic torque
J_{GB21}	Gearbox 21 damping	F_T	Wind thrust
J_{GB22}	Gearbox 22 damping	K_T	Tower stiffness
N_{GB1}	Gearbox ratio	D_T	Tower damping
N_{GB2}	Gearbox ratio		

A picture of two-mass gearbox model is shown in Figure 4. There are numerous forms of gearbox structures, classifying from one-mass model to six-mass model. In this study, the assumption for using a two-mass model is adequate.

By using the second of Newton principle on revolving rule, picture of wind power turbine model in Figure 4 would be get through with differential equations.

$$T_a = J_H\ddot{\omega}_H + D_{HGB}\dot{\Phi}_\Delta + K_{HGB}\phi_\Delta \tag{1}$$

$$m_T = F_T + D_T\dot{z} + K_T z \tag{2}$$

$$-T_{em}N_G = J_G N_G^2 \frac{\dot{\omega}_G}{N_G} - D_{GBG}\dot{\Phi}_\Delta - K_{GBG}\phi_\Delta \tag{3}$$

where $\phi_\Delta = \phi_H - (\phi_G/N_G)$ and $\dot{\phi}_\Delta = \omega_H - (\omega_G/N_G)$. In a thoroughly elemental method, a mechanical structure of wind turbine model can be converted in Figure 4 hooked up Bond-graph description, as shown in Figure 5. Because of a dynamic characteristic exists in between their inertias, they do not possess an identical velocity. This is a purpose to utilize the *0*-junction, since the rotating forces have the same value by supposing there is no loss calculated in a gearbox. The *1* junction linked to resistive and passivity elements entitle revolving speed distinction among both inertias and also shows that compliance and resistive elements possess same rotational speed, but difference torque. This system is able to be simplified as shown in Figure 6.

From Bond-graph based wind turbine without induction generator, there will be ten of dynamic elements, namely six inertias, two of springs and dashpots. First order differential equations can be created as (4), (5), (6)

$$\dot{p}_2 = e_2 = e_1 - e_3 = T_a - (q_5/C_5) - R_5 f_5 \tag{4}$$

$$\dot{q}_5 = f_5 = f_3 - f_7 = (p_2/I_2) - N_g(p_9/I_9) \tag{5}$$

$$\dot{p}_9 = e_9 = e_8 + e_{10} = -T_e + (1/N_g)((q_5/C_6) + R_5 f_5) \quad (6)$$

Obviously, equations (4), (5), and (6) are accurately the same as (1) and (3) through some mathematical manipulations.

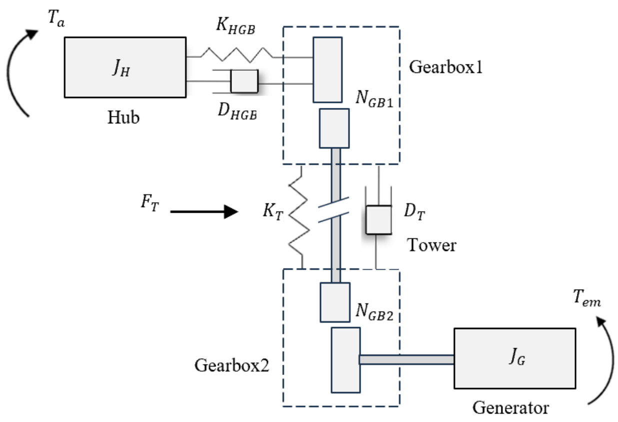

Figure 4. Drawing of wind turbine with gearbox and induction generator model

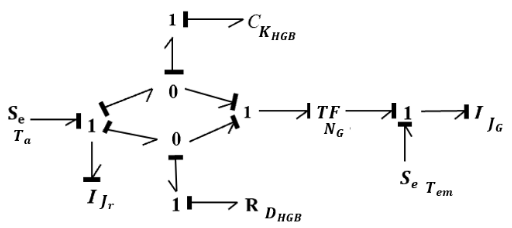

Figure 5. Bond-graph based blade and gearbox 1 model

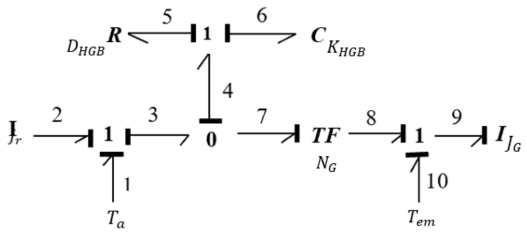

Figure 6. Simplification of Bond-graph based blade and gearbox 1 model

The tower movement is supposed to have no effect on the mechanical structure, it just influences its input, such as a wind thrust. Bond-graph structure of tower movement is shown in Figure 7. Initial line to create Bond-graph based model is earliest recognizing what kind of components involvement corresponding *flow* or *effort*. Spring and damper are the link between hub and the ground. It is supposed zero input force after the ground; each time passing bonds exist on a junction, they are able to be removed. Figure 8 explains simplification process of Figure 7. An equation from Bond-graph based tower movement model is

$$\dot{p} = S_e - R\frac{p_2}{I} - \frac{q_3}{C} \quad (7)$$

$$\dot{q}_3 = \frac{\dot{p}_2}{I} \quad (8)$$

Equation (8) can be recomposed in a non-Bond-graph representation

$$m_t\ddot{z} = F_t - D_t\dot{z} - K_t z \quad (9)$$

where m_T is a tower mass, and F_T, D_T and K_T are tower working force, damping and stiffness, respectively.

Bond-graph based induction generator linked blade over gearbox model denoting the mechanical structure can be shown in Figure 9. At this point, wind thrust along with generator torque and tower movement towards every blade become an input. The thrust of wind is running into and out of a modulated gyrator that converts *flow* into *effort* corresponding to method set in within a gyrator. This conversion hooked on blades' pitch angle; consequently, this is a kind of modulated gyrator. This could be recognized such every *R*, *I* or *C* component comprises an identical causality, correspondingly. All elements have their chosen causality. The causality of the *R* component is not that significant as it is not a dynamic element.

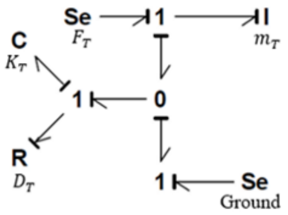

Figure 7. Bond-graph based tower movement

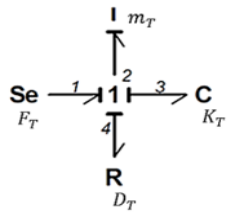

Figure 8. Simplified Bond-graph based tower movement

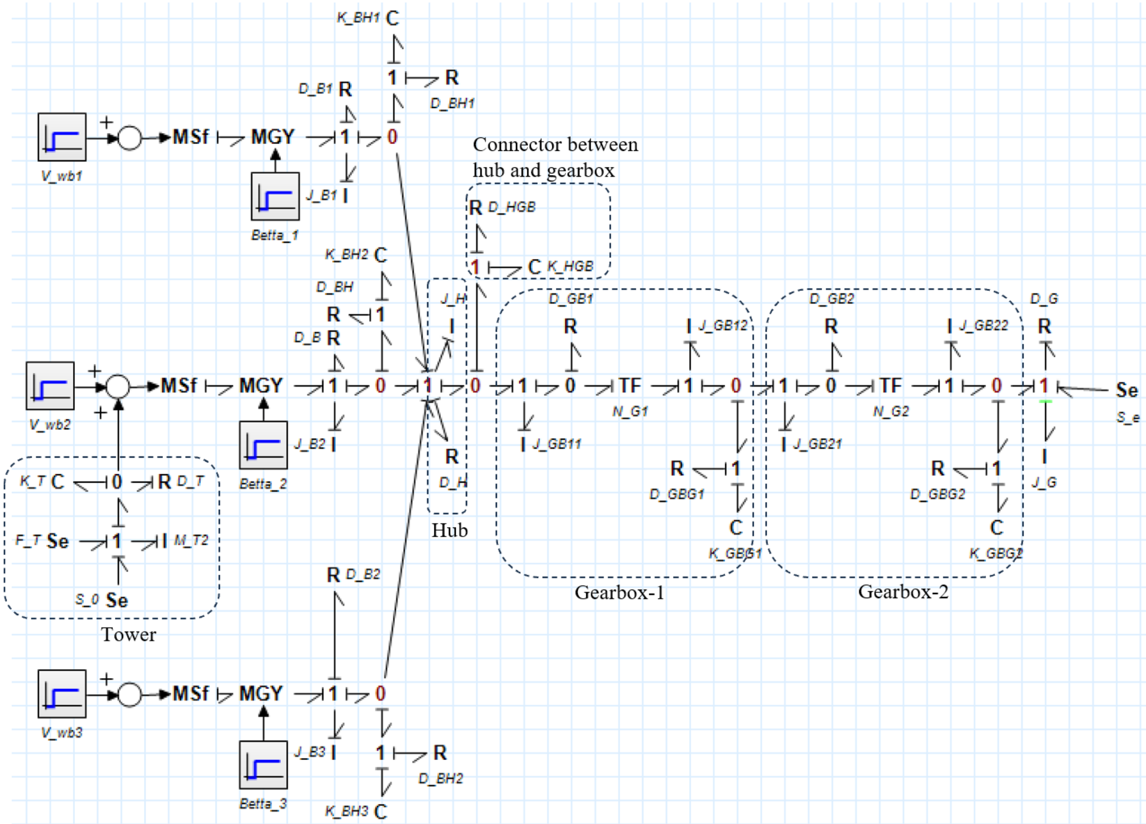

Figure 9. Bond-graph based wind turbine without induction generator model

2.2. Bond-graph structure of singly-fed induction generator

Stator, rotor or shaft becomes energy *port* within singly-fed induction generator. Stator picks-up energy delivery out of the centrals; rotor can be come up with electric energy from centrals concerning generator or divide energy by stator. Shaft transfers energy to the power consumer. Air gap is a location where conversion process among the *ports* considering energy taken place [17].

The mathematical equation of 3 phases singly-fed induction generator will be a fifth order non-linear differential function [18], [19]. In [20], [21] suggests a Bond-graph structure for describing aforementioned function. Structures might be embodied in two common styles, namely those which use Park's reference of frame and others which use natural reference of frame. Bond-graph based singly-fed induction generator model within Park's reference of frame is exposed in Figure 10 [22]–[24]. The hypothesis observed for generator that joint inductances covering framework and *amortisseur* wirings, along with field around direct-axis wirings have identical value is theory of generator concept. Besides, losses of copper and generator slots are unnoticed. Stator fluxes spreading and apertures travel are sine wave figures. *Amortisseur* windings sitting nearly by air wall exhibit flux involving damper wirings with similar value as flux linking armature.

To describe physical system elements clearly, certain Bond-graph components should be augmented. In Figure 11, α and β are phase stator resistance elements; then, $R_{s\alpha}$ and $R_{s\beta}$ need to be ripped into three stator winding resistances, R_{sa}, R_{sb}, and R_{sc}, to build an explicit resistance of every stator coils.

This was accomplished without changing the prevailing equivalences which is under hypothesis of geometrical sine wave distribution of magnetomotive forces and ignoring both losses and saturation of magnetics.

$$\begin{bmatrix} V_{\alpha s} \\ V_{\beta s} \\ 0 \\ 0 \end{bmatrix} = \begin{bmatrix} R_s + L_s\,d/dt & 0 & L_m\,d/dt & 0 \\ 0 & R_s + L_s\,d/dt & 0 & L_m\,d/dt \\ L_m\,d/dt & L_m\omega_r & R_r + L_r\,d/dt & L_r\omega_r \\ -L_m\omega_r & L_m\,d/dt & -L_r\omega_r & R_r + L_r\,d/dt \end{bmatrix} \begin{bmatrix} i_{\alpha s} \\ i_{\beta s} \\ i_{\alpha r} \\ i_{\beta r} \end{bmatrix} \tag{10}$$

Equation (9) connects stator voltages to currents of both stator and rotor. Furthermore, the necessary is rotating force of electromagnetic motor for a P-pole type of machine, stated in place of 10.

$$T_{em} = \frac{P}{2}\left[I_{\alpha s}\left(L_m I_{\beta s} + L_r I_{\beta r}\right) - I_{\beta r}\left(L_m I_{\alpha s} + L_r I_{\alpha r}\right)\right] \tag{11}$$

This motor torque is well-adjusted compared to additional torques through

$$T_{em} = J\frac{d\omega_m}{dt} + c\omega_m + T_L \tag{12}$$

Terms of (10) to (12) denote torques of rotor inertial, shaft damping, and load, respectively. $V_{\alpha s}$ and $V_{\beta s}$ represent α and β axis stator voltages; $i_{\alpha s}$ and $i_{\beta s}$ signify α and β axis stator currents; $i_{\alpha r}$ and $i_{\beta r}$ are α and β axis rotor currents. R_s, R_r, L_s, L_r and L_m are resistances and individually inductances of both stator and rotor, and joint inductance, respectively. T_e is electromagnetic torque and T_L mechanical load torque, correspondingly. Then J, c, v_r, v_m and P are sluggishness moment of rotor, constant of gluey resistance, electrical and angular speeds of rotor, and pole couples' quantity, respectively.

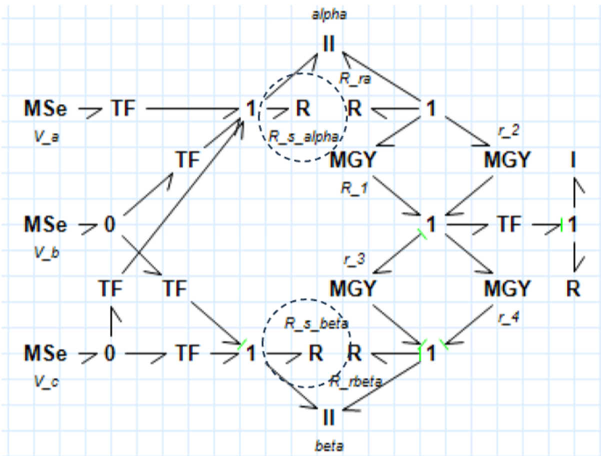

Figure 10. Structure of Ghosh and Bhadra's Bond-graph based induction generator model [25]

Figure 11 utilized modulated gyrators $MGY{:}r_1 = L_m I_{\beta s}$, $MGY{:}\ r_2 = L_r I_{\beta r}$, $MGY{:}\ r_3 = L_m I_{\alpha s}$, $MGY{:}\ r_4 = L_r I_{\alpha r}$ to signify the electromagnetic torque of (11) and used transformers $TF{:}m_1$, $TF{:}m_2$, $TF{:}m_3$, $TF{:}\ m_4$, and $TF{:}m_5$ with moduli $m_1 = (3/2)^{1/2}$, $m_2 = m_3 = -(6)^{1/2}$, $m_4 = (2)^{1/2}$, and $m_5 = -(2)^{1/2}$ to apply the mathematical change and stimulated scheme with *effort* sources, *MSe*:V_a , *MSe*:V_b , and *MSe*:V_c, taking sine wave voltages by means of identical amplitudes but 0, *p*/3, and *2p*/3 phase laggings, respectively. While that appropriately arranging principal calculations for 3 phases motor, components and basic laws involve energy domains of electrical and mechanical. Conceive parameters applicable to magnetic area stay be involved within reciprocated inductances, enquired as 2-port inertances $I{:}\alpha$ also $I{:}\beta$ through basic rules.

$$\begin{bmatrix} \lambda_{\alpha s} \\ \lambda_{\alpha r} \end{bmatrix} = \begin{bmatrix} L_s & L_m \\ L_m & L_r \end{bmatrix} \begin{bmatrix} i_{\alpha s} \\ i_{\alpha r} \end{bmatrix} \qquad \begin{bmatrix} \lambda_{\beta s} \\ \lambda_{\beta r} \end{bmatrix} = \begin{bmatrix} L_s & L_m \\ L_m & L_r \end{bmatrix} \begin{bmatrix} i_{\beta s} \\ i_{\beta r} \end{bmatrix} \tag{13}$$

Within $\lambda_{\alpha s}$, $\lambda_{\beta s}$, $\lambda_{\alpha r}$, and $\lambda_{\beta r}$ denote flux connections of the corresponding coiling.

An advanced Bond-graph structure is shown in Figure 12 which moved $R_{s\alpha}$ and $R_{s\beta}$ back-over the transformers before the phases. To preserve a similarity among Figures 11 and 12, R_{sa}, R_{sb}, and R_{sc} are related to R_{sa} and R_{sb}. Since induction generator has symmetry between phases, so $R_{sa} = R_{sb} = R_{sc} = R$ and $R_{s\alpha} = R_{s\beta} = R_s$. For the Bond-graph of Figures 11 and 12 to be comparable, the voltages (acts as an *efforts*) on 2-port inertances by stator parts are the same. Causality seen at Figures 11 and 12 declare such the voltages to the 2-port inertances develop among an adjacent 1-junctions. Adding voltages as of more bonds to these 1-junctions, and linking the aforementioned voltages between Figures 11 and 12 creates

$$\frac{V_a}{m_4} + \frac{V_c}{m_5} - R_s i_{\beta s} = \frac{1}{m_4}\left\{V_b - R\left(\frac{i_{\alpha s}}{m_2} + \frac{i_{\beta s}}{m_4}\right)\right\} + \frac{1}{m_5}\left\{V_c - R\left(\frac{i_{\alpha s}}{m_3} + \frac{i_{\beta s}}{m_5}\right)\right\} \tag{14}$$

$$\frac{V_a}{m_1} + \frac{V_b}{m_2} + \frac{V_c}{m_3} - R_s i_{\alpha s} = \frac{1}{m_1}\left\{V_a - R\left(\frac{i_{\alpha s}}{m_1}\right)\right\} + \frac{1}{m_2}\left\{V_b - R\left(\frac{i_{\alpha s}}{m_2} + \frac{i_{\beta s}}{m_4}\right)\right\} + \frac{1}{m_3}\left\{V_c - R\left(\frac{i_{\alpha s}}{m_3} + \frac{i_{\beta s}}{m_5}\right)\right\} \tag{15}$$

Through explaining for $i_{\beta s}/i_{\alpha s}$ will be obtanined equations in respect of resistances and transformer moduli

$$\frac{i_{\beta s}}{i_{\alpha s}} = \frac{(m_3 m_4 m_5^2 + m_2 m_4 m_5^2)R}{m_2 m_3 m_4^2 m_5^2 R_s - (m_2 m_3 m_5^2 + m_2 m_4 m_5^2)R} =$$

$$\frac{m_1^2 m_2^2 m_3^2 m_4 m_5 R_s - (m_2^2 m_3^2 m_4 m_5 + m_1^2 m_3^2 m_4 m_5 + m_1^2 m_2^2 m_4 m_5)R}{(m_1^2 m_2 m_3^2 m_5 + m_1^2 m_2^2 m_3 m_4)R} \tag{16}$$

By swapping the transformer moduli, m_1 to m_5 of 3 phases into 2 phases transformation with real numbers, $m_1 = (3/2)^{1/2}$, $m_2 = m_3 = -(6)^{1/2}$, $m_4 = (2)^{1/2}$, and $m_5 = -(2)^{1/2}$, given in (17).

$$\begin{bmatrix} i_\alpha \\ i_\beta \end{bmatrix} = \frac{\sqrt{2}}{\sqrt{3}} \begin{bmatrix} \cos 0 & \cos 2\pi/3 & \cos 4\pi/3 \\ \sin 0 & \sin 2\pi/3 & \sin 4\pi/3 \end{bmatrix} \begin{bmatrix} i_a \\ i_b \\ i_c \end{bmatrix} \tag{17}$$

It will be found that $R_s = R$; particularly $R_{s\alpha} = R_{s\beta} = R_{sa} = R_{sb} = R_{sc}$.

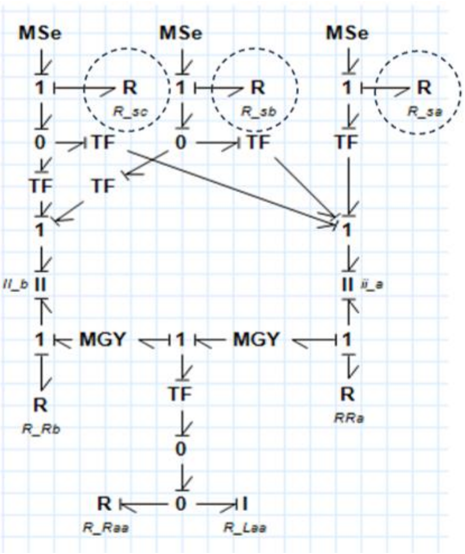

Figure 11. Park's reference of frame of singly-fed induction generator

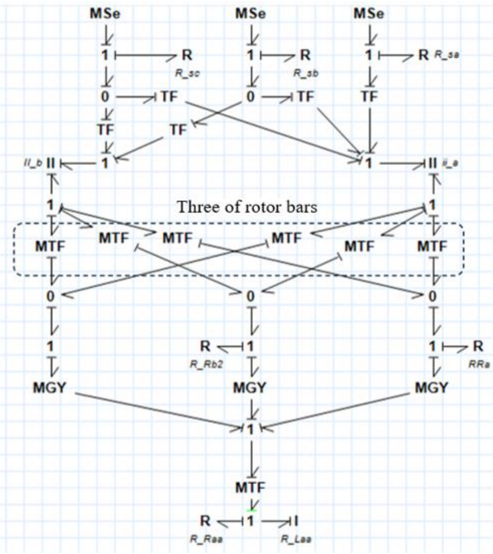

Figure 12. Transformation of phase currents, α and β, into bar currents, and insertion of rotor bar activity

The Bond-graph model at Figure 13 describes relationship among stator windings and rotor bars in 2-port I-components shapes within electric energy area. The model contains three of rotor bars and inductance defining magnetic energy storage and ignores magnetic leakage and power loss. Losses and leakage powers which are generated at magnetic area that could be triggered through worsening elements are omitted.

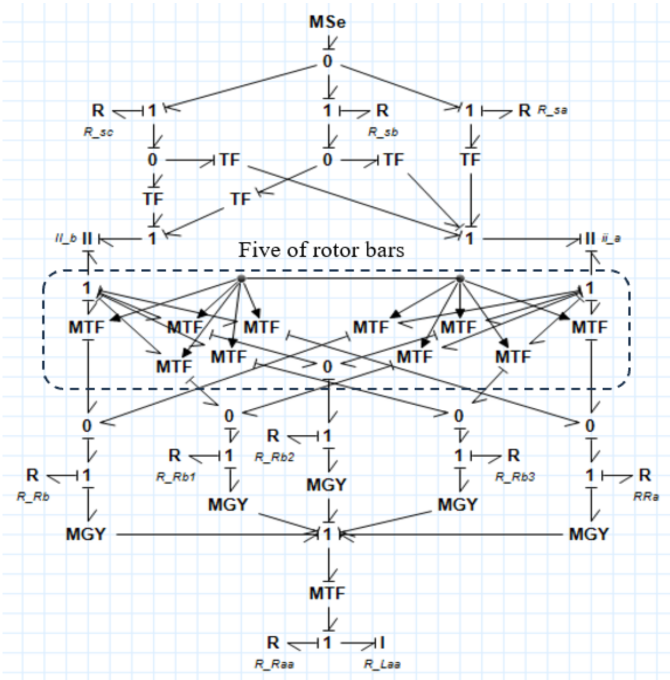

Figure 13. Bond-graph model showing both stator and rotor bar actions within magnetic circuit

2.3. Bond-graph structure of doubly-fed induction generator

Induction generator is made up of 6 electromagnetically linked windings running through rotor orientation, as shown in Figure 14. Instantaneous voltage of each winding owns an outline corresponding.

$$v = \pm \sum ri \pm \lambda \tag{18}$$

where λ, r, and i denote flux linking, winding resistance, and currents moving on or after *ports*, correspondingly. Simplified mathematical explanation of the induction generator is ended from the Park's conversion. The Park's conversion alters numbers of entirely stator *a*, *b*, and *c* phases tided on current parameters of frame reference of things that rotates with rotor. The Park's conversion is

$$P = \sqrt{\frac{2}{3}} \begin{bmatrix} \frac{1}{\sqrt{2}} & \frac{1}{\sqrt{2}} & \frac{1}{\sqrt{2}} \\ \cos\theta & \cos\left(\theta - \frac{2\pi}{3}\right) & \cos\left(\theta + \frac{2\pi}{3}\right) \\ \sin\theta & \sin\left(\theta - \frac{2\pi}{3}\right) & \sin\left(\theta + \frac{2\pi}{3}\right) \end{bmatrix} \tag{19}$$

The model of Figure 15 illustrates Bond-graph structure of induction generator in Park's transformation [24]–[28]. A random *dq*-frame revolving nearby all over non-polar *0*-axis prior to speed ω_s was chosen. Equations defining Bond-graph structure are given by (20)

$$\begin{aligned} v_d &= R_s i_{sd} + \frac{d\varphi_{sd}}{dt} - \omega_s \varphi_{sq} & \qquad v_d &= R_s i_{sd} + \frac{d\varphi_{sd}}{dt} - \omega_s \varphi_{sq} \\ v_{rd} &= R_d i_{rd} + \frac{d\varphi_{rd}}{dt} - \omega_s \varphi_{rq} + p\Omega\varphi_{rq} & \qquad v_{rq} &= R_r i_{rq} + \frac{d\varphi_{rq}}{dt} - \omega_s \varphi_{rd} + p\Omega\varphi_{rd} \\ \tau_{11} &= p(\varphi_{rq} - \varphi_{rd}) & \qquad \tau_{11} &= J_m \frac{d\Omega}{dt} - T_m \end{aligned} \tag{20}$$

The *I*-field inductance matrices, M_d and M_q, permit connection between both stator and rotor fluxes through the equation displayed within

$$\begin{pmatrix} \varphi_{sd/q} \\ \varphi_{rd/q} \end{pmatrix} = \begin{pmatrix} L_s & L_m \\ L_m & L_r \end{pmatrix} \begin{pmatrix} i_{sd/q} \\ i_{rd/q} \end{pmatrix} \tag{21}$$

where L_s, L_m, and L_r are individually inductance of stator, joint inductance between stator and rotor, and individually inductance of rotor, respectively. I-field component and J_m, are shaft and rotor moment of inertias. While R_s, R_r, and p are resistances of stator and rotor, and pole pairs number, respectively; ω relates on $2\pi f$.

Modulated sources that sort out along ω_s denote implicit sources, since aggregate of powers are equal to zero and just algebraic effect of the model. Everything is viewed through the arbitrary framework hypothesis and are able to be eliminated if a fixed frame is selected by putting d-axis by stator phase a because the value of $\omega_s = 0$. Utilizing the model concerning rotor and stator equations are not affected by means of rotor speed.

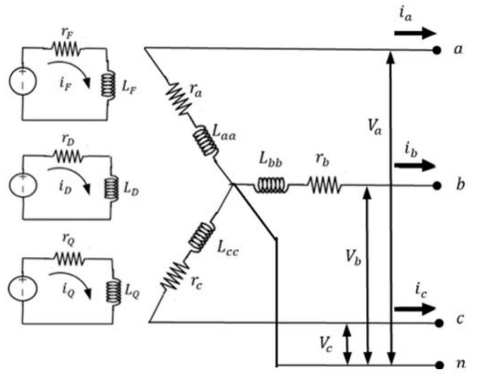

Figure 14. Graphic illustration of induction generator structure

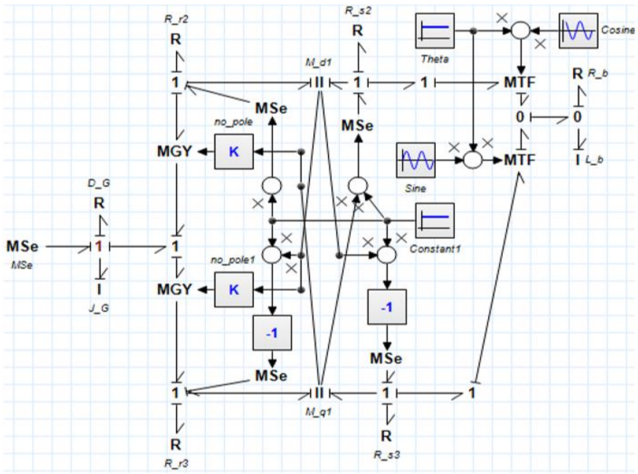

Figure 15. Park's reference frame of Bond-graph based doubly-fed induction generator [29]

3. RESULTS AND DISCUSSION

For the purpose of comparing behavior of the singly-fed against the doubly-fed induction generators, simulations are accomplished by considering circumstances of wind speeds, namely steady and variable speeds. The rate of steady speed is 2 m/s, while values of variable wind speeds are changing between 1.5 m/s and to 2.5 m/s. Table 2 shows the parameters for both types of induction generators.

Table 2. The induction generators parameters [30], [31]

Components	Rated	Components	Rated
Power	2.5 kW	Stator resistance	2.30 Ω
Voltage	220/380 V	Rotor resistance	6.95 Ω
Pole pairs	2	Stator inductance	0.040 H
Speed	1420 rpm	Rotor inductance	0.036 H
Moment of inertia	0.2 kg.m^2	Mutual inductance	0.061 H

The set-up for simulation is in that manner: steady wind of 2 mps (meter per second) is used in process of simulation. The system consists of 2.5 kW wind turbines is connected to a tower and a two-mass gearbox system to a *RL* load. The 2.5 kW wind turbine is simulated by three blades turbines of each 3 m diameter. The induction generators are singly-fed induction generator which consists of three of rotor bars and ignores magnetic leakage and power loss actions. The blades, gearbox, tower, and induction generators are related as means to express the thorough model of a constant and variable speeds of the wind. Simulation reactions intend for wind speed, induction generator speed, and stator current of generator, respectively. The simulations are held by backward differentiation rule of 20-Sim and use absolute integral error of 0,00001 [32].

Figure 16 shows the simulation of singly-fed induction generator model with a constant wind speed. Over that time frame, turbine speed will remain at speed 2 mps, shown in Figure 17. We will observe that the singly-fed induction generator speed reaches steady-state in approximately 4.1 seconds, as shown in Figure 17. Compared with steady wind, stator currents decline to constant value, while speed oscillation of generator is disappeared. Stator currents fluctuate at the input frequency with early huge magnitude, their response reflects their variability with wind, from 46.376 p.u. to 86.926 p.u., as shown in Figure 17.

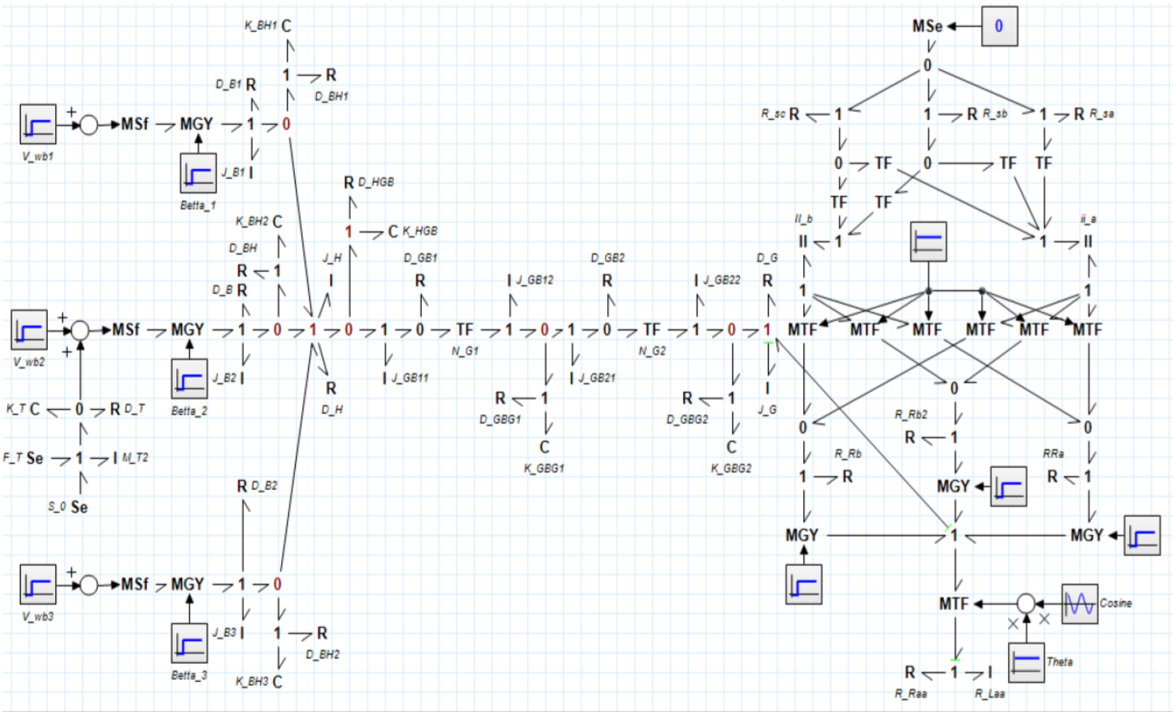

Figure 16. Simulation of Bond-graph structure of singly-fed induction generator model under steady wind speed, inserting three of rotor bars and exclusion of magnetic leakage and power loss actions

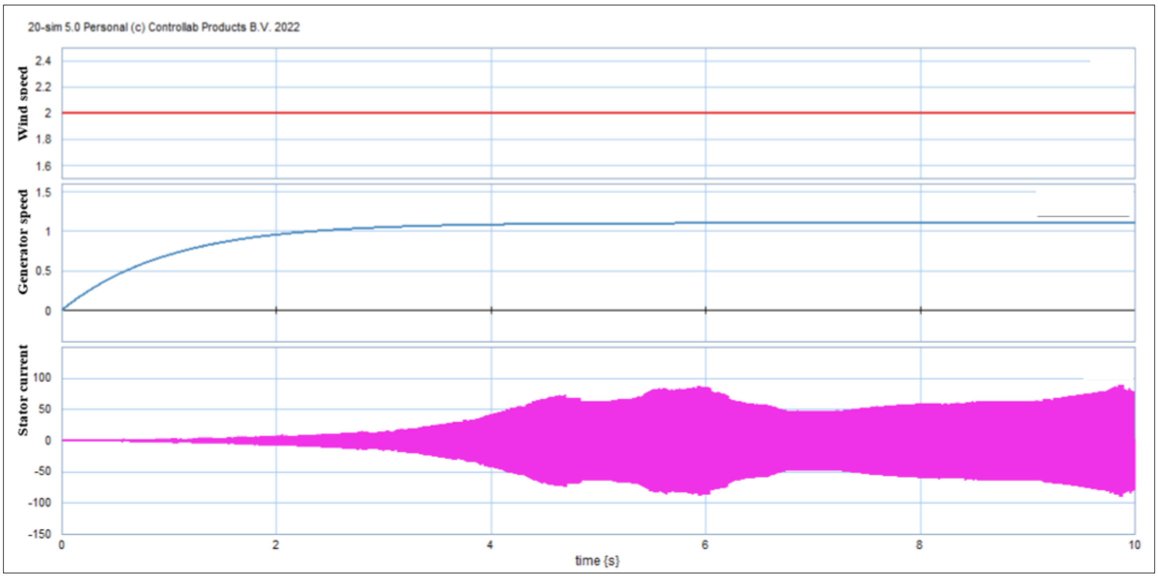

Figure 17. Steady speed performance of wind: wind speed, machine speed, and stator current

Model of Figure 18 describes the simulation of 3 phases of singly-fed induction generator with constant wind speed; R_S and R_r and *IC*-port field describes L_s, L_r, and L_m. Simulation has been conducted under: i) Singly-fed induction machine used as generator (input torque is negative) and ii) *RL* load (0.0014, 0.0045 p.u.) is linked to a singly-fed induction generator of 2.5 kW, 220/380 V at 50 Hz.

Figure 19 displays turbine speed at 2 mps. It will be observed that the singly-fed induction generator speed which inclusion of five of rotor bars action increases from 0 p.u. to steady-state condition in approximately 4.5 seconds, shown in Figure 19. Meanwhile, current response reproduces their variability with wind, from 77.864 p.u. to 138.658 p.u., as shown in Figure 19.

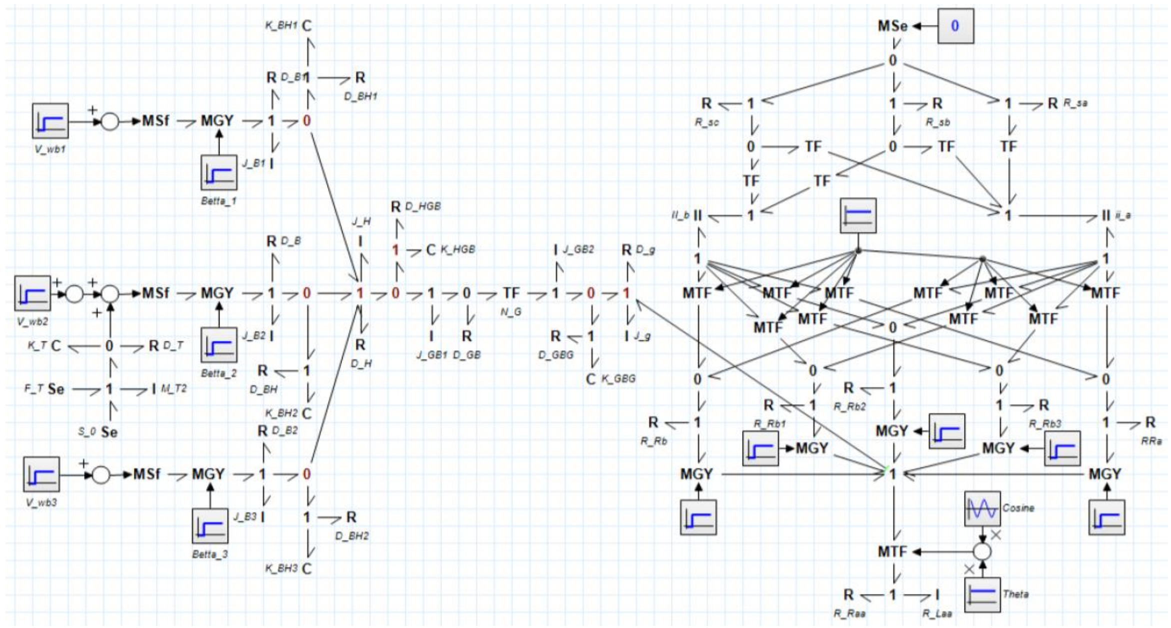

Figure 18. Simulation of Bond-graph structure of singly-fed induction generator under steady wind speed, inserting five of rotor bars and exclusion of magnetic leakage and power loss actions

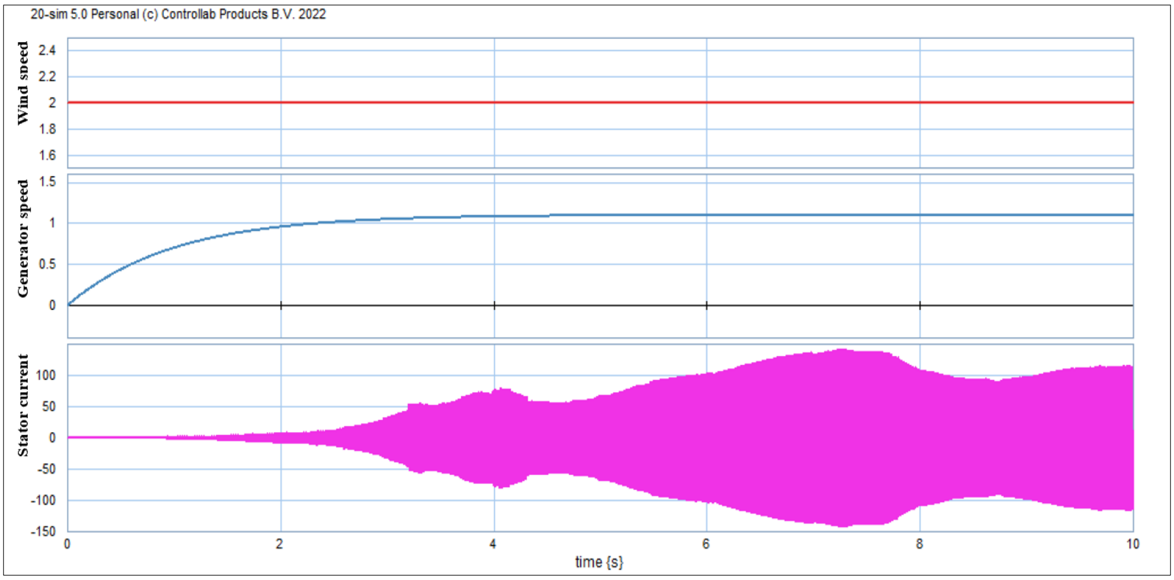

Figure 19. Performance for steady speed of wind: wind speed, machine speed, and stator current

Comparing Figures 19 to 17, we found that the stator current output value is proportional to amount of rotor bars contained in the induction generator. The greater the amount of rotor bars, the higher the value of the generator stator current output. Under these conditions, the steady state time interval will be longer, from 4.1 p.u. to 4.5 p.u., shown in Figures 17 and 19.

As a means to confirm a response of singly-fed induction generator with variable wind profile, a simulation is implemented by applying singly-fed induction generator as main governor to exceed the torque supplied via variable speed of the blade. As well, in point of fact that the load takes significant influence in generator performance. She simulation of Bond-graph singly-fed induction generator model comprises tower and two of gearboxes; and variable wind trust are added.

Turbine speed will vary starting with 1.5 mps until 2.5 mps, shown in Figure 20. It will be observed that the generator speed increases from 0 p.u. to until steady-state in approximately 5.8 seconds, as shown in

Figure 20. In contrast to variable wind input, from 1.5 mps to 2.5 mps, current response reflects their variability with wind, from 60.091 p.u. to 104.796 p.u., seen in Figure 20.

Comparing Figures 20 to 19, we found stator current output of generator is proportional to the wind speed quantity. Greater wind speed will increase stator current output. Under these conditions, the steady state time interval will be longer, changing from 4.5 p.u. to 5.8 p.u., seen in Figures 19 and 20.

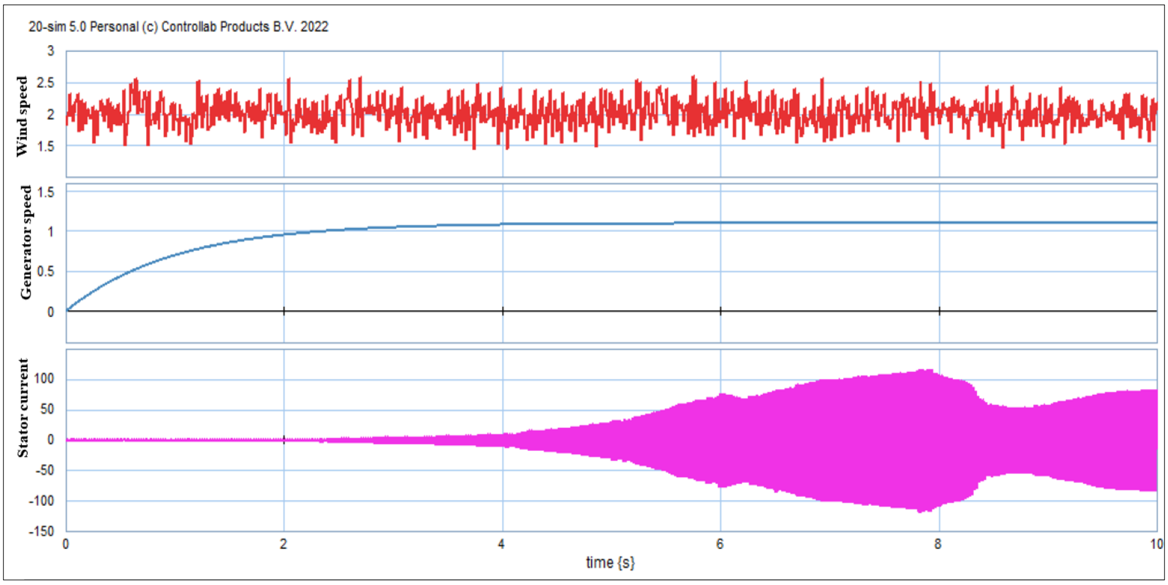

Figure 20. Performance for variable speed of wind: wind speed, machine speed, and stator current

Figure 21 displays the simulation shape of Bond-graph based doubly-fed induction generator model. Figure 22(a) shows those responses of each step changes with wind (namely 2 m/s). This permits the performance to be verified by the suggested model. In distinction to a constant wind input, current response reflects their variability with wind.

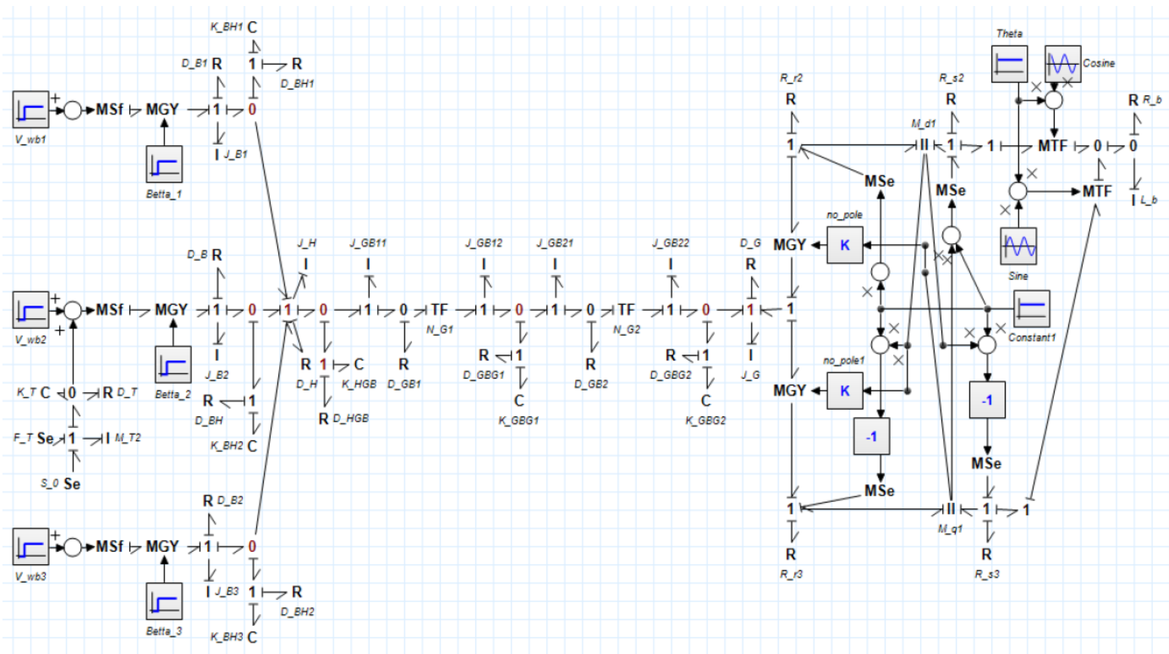

Figure 21. Simulation of Bond-graph structure of doubly-fed induction generator under steady wind speed

At Figure 22(a), 1 by blade radius of 1.5 m, the rate speed of hub reaches nearly 1.33 rad/s. Speed of generator increases equivalently as well as wind speed. The speed achieves its nominal value of 157.10 rad/s due to steady-state circumstance within an interval of 5.72 second. The stator current of generator varies slightly around 71.066 p.u., shown in Figure 22(a).

With respect to verify reaction of generator for variable wind profile, a simulation is applied by generator as main controller to exceed rotating force delivered through variable speed of the blade. Also, as it is assed that the load has a significant influence in the generator performance. Figure 22(b) displays wind is running in around 1.5 mps and 2.5 mps. At Figure 22(b), with blade radius of 1.5 m, rotor speed of generator escalates equivalently with wind speed. The speed of generator catches its nominal value of 157.08 rad/s and it is attained at 4.66 second, the same as the condition that the wind speed remains equal to 2 m/s. Figure 22(b) states that stator current fluctuates at the same value under constant wind speed conditions, namely at ambient around 71.066 p.u.

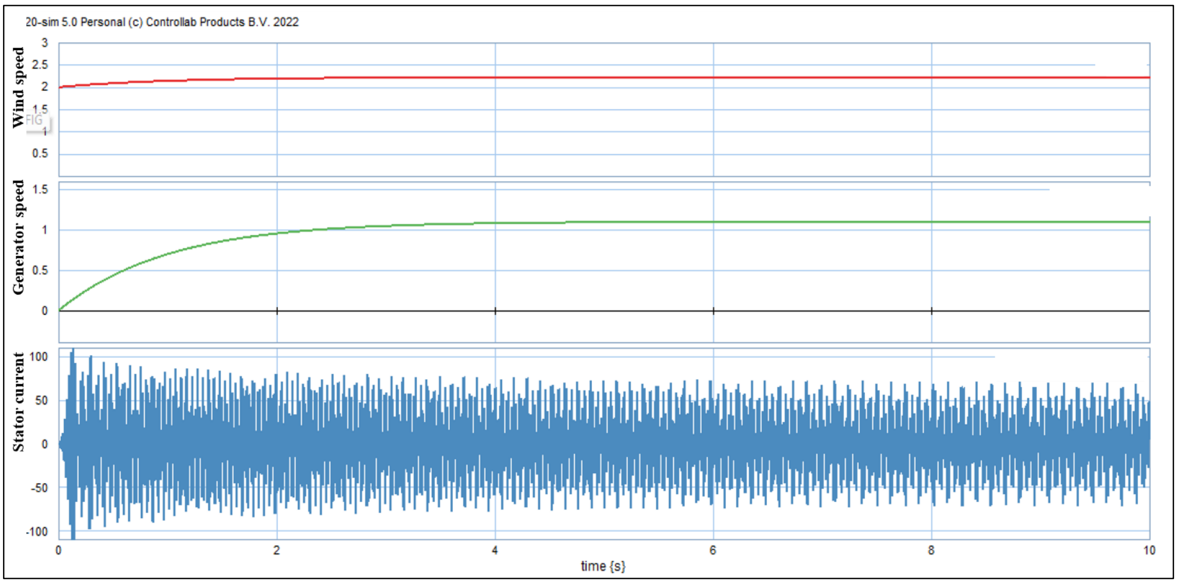

(a)

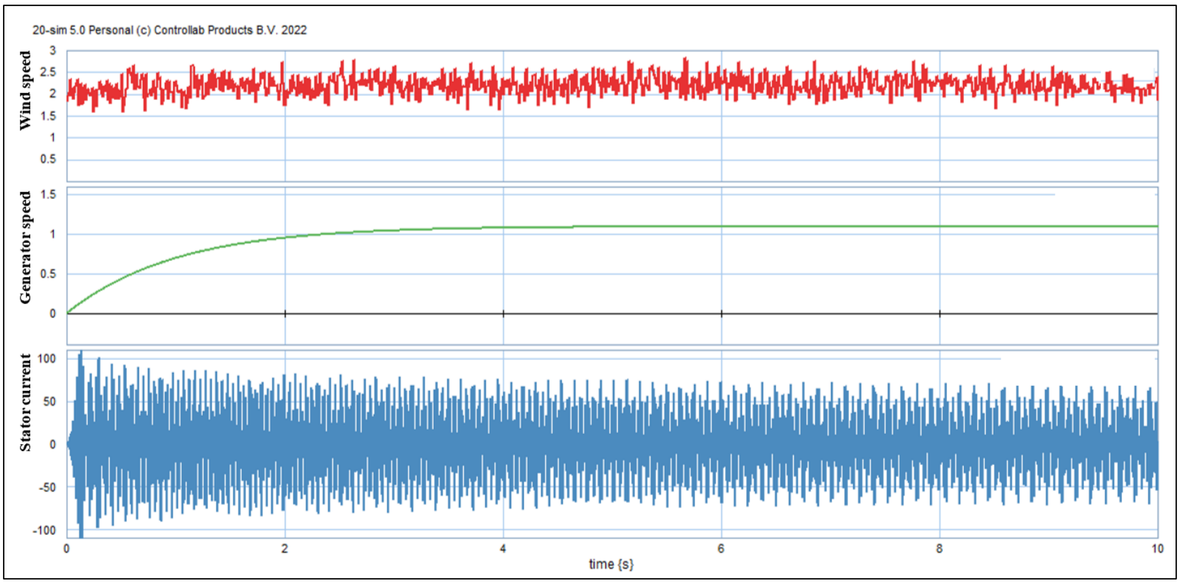

(b)

Figure 22. Performance of wind speed, machine speed, and stator current (a) steady wind speed and (b) variable wind speed

Comparing Figure 22(b) to both Figure 22(a) and Figure 20 will provide conclusive evidence that this adjustable speed operation of doubly-fed induction generator decreases mechanical stresses as energy of wind gusts is kept in mechanical inertia of turbine blade. It will produce a flexibility that decreases torque vibrant and therefore improving the quality of power. This also upgrades system efficiency as turbine speed is adapted as wind speed function as so to increase the output power. Meanwhile, a singly-fed induction generator cannot adapt the performance of variable speed of wind.

4. CONCLUSION AND UPCOMING WORK

Comprehensive Bond-graph structures of wind turbines have been suggested. With the aim of applying aerodynamic force, the structure of blades should be counted as an elastic body. The momentum theory of blade element is applied to convert an aerodynamic force of the wind. The rates of rotating force and current magnitude in simulations have seen validity of the proposed model. In opposition to a constant wind input, current response of singly-fed induction generator reflects their variability with wind, from 46.376 p.u. to 86.926 p.u. during steady speed, such as 2 mps. When speed of wind is vary increasing since 1.5 mps until 2.5 mps then current response varies from 60.091 p.u. to 104.796 p.u. On the contrary, whether under steady (namely 2 mps) or varying wind speeds (between 1.5 mps and to 2.5 mps) conditions, performance of speed and stator current generators tend to remain constant; steady state nominal of generator speed is 157.08 rad/s (at 4.66 seconds) and stator current varies at ambient around 71.066 p.u.

Doubly-fed induction generator system exhibits better current quality as compared to singly-fed induction generator. This variable speed operation degrades mechanical stresses as energy of rushes of wind is accumulated in mechanical inertia of turbine, creating a flexibility that decreases torque pulsation. Moreover, it will improve the quality of output current. As a future work, this Bond-graph based wind turbine model will be supplemented with the control techniques originated by the model and utilizing bi-casualty conception. The moment the power control method is included. Supplementary elements which is essential within wind turbine, namely stator active power control and reserve apparatus, would be combined with the purpose of signifying the complete system.

ACKNOWLEDGEMENTS

The author would like to expresses his thanks to Directorate of Research, Technology, and Community Service, Director General of Higher Education, Research and Technology, Ministry of Education and Culture, Research and Technology who fully funded the research of wind turbine design with DFIG Configuration under subsidy no. 181-E5-PG-02-00-PL-2023, and 0423-25-LL5-INT-AL.-04-2023.

REFERENCES

[1] L. Hunter and M. Ahmad, *Expectations for renewable energy finance in 2023-2026: how companies are realizing the post-IRA opportunity while navigating headwinds*. American Council on Renewable Energy (ACORE), 2023.

[2] REN21, "Renewables 2023 global status report collection, renewable energy systems and infrastructure," REN21, Paris, France, 2023. https://www.ren21.net/gsr-2023/modules/energy_systems_infrastructure/ (accessed Oct 29, 2023).

[3] K. K. Jaiswal *et al.*, "Renewable and sustainable clean energy development and impact on social, economic, and environmental health," *Energy Nexus*, vol. 7, Sep. 2022, doi: 10.1016/j.nexus.2022.100118.

[4] T.-Z. Ang, M. Salem, M. Kamarol, H. S. Das, M. A. Nazari, and N. Prabaharan, "A comprehensive study of renewable energy sources: Classifications, challenges and suggestions," *Energy Strategy Reviews*, vol. 43, Sep. 2022, doi: 10.1016/j.esr.2022.100939.

[5] J. M. Akanto, M. K. Islam, E. Jahan, M. R. Hazari, M. A. Mannan, and M. A. Rahman, "Dynamic analysis of grid-connected hybrid wind farm," *International Journal of Power Electronics and Drive Systems (IJPEDS)*, vol. 14, no. 2, pp. 1230–1237, Jun. 2023, doi: 10.11591/ijpeds.v14.i2.pp1230-1237.

[6] J. Brunarie, G. Myerscough, A. Nystrom, and J. Ronsen, "Delivering cost savings and environmental benefits with hybrid power," in *INTELEC 2009 - 31st International Telecommunications Energy Conference*, Oct. 2009, pp. 1–9, doi: 10.1109/INTLEC.2009.5351778.

[7] Z. Al-Omari and W. Emar, "Modeling and simulation of a stand-alone wind turbine supplying an inductive load through a long cable," *International Journal of Power Electronics and Drive Systems (IJPEDS)*, vol. 13, no. 3, pp. 1654–1665, Sep. 2022, doi: 10.11591/ijpeds.v13.i3.pp1654-1665.

[8] A. Bensalah, M. A. Benhamida, G. Barakat, and Y. Amara, "Large wind turbine generators: state-of-the-art review," in *2018 XIII International Conference on Electrical Machines (ICEM)*, Sep. 2018, pp. 2205–2211, doi: 10.1109/ICELMACH.2018.8507165.

[9] Y. Zou, "Induction generator in wind power systems," in *Induction Motors - Applications, Control and Fault Diagnostics*, InTech, 2015.

[10] A. K. Abdulabbas, M. A. Alawan, and D. K. Shary, "Limits of reactive power compensation of a doubly fed induction generator based wind turbine system," *Bulletin of Electrical Engineering and Informatics (BEEI)*, vol. 12, no. 5, pp. 2521–2534, Oct. 2023, doi: 10.11591/eei.v12i5.4968.

[11] S. Kharoubi and L. El Menzhi, "Wind turbine doubly-fed induction generator defects diagnosis under voltage dips," *TELKOMNIKA (Telecommunication Computing Electronics and Control)*, vol. 20, no. 5, pp. 1159–1171, Oct. 2022, doi: 10.12928/telkomnika.v20i5.23760.

[12] W. Borutzky, "Bond graph based physical systems modelling," in *Bond Graph Methodology*, London: Springer London, 2010, pp. 17–88.

[13] J. Kypuros, *System dynamics and control with bond graph modeling*. CRC Press, 2013.
[14] P. C. Breedveld, "Concept-oriented modeling of dynamic behavior," in *Bond Graph Modelling of Engineering Systems*, New York, NY: Springer New York, 2011, pp. 3–52.
[15] A. Gambier, "Dynamic modelling of the rotating subsystem of a WT for controller design purposes," *IFAC-PapersOnLine*, vol. 50, no. 1, pp. 9896–9901, Jul. 2017, doi: 10.1016/j.ifacol.2017.08.1621.
[16] S. M. Muyeen *et al.*, "Comparative study on transient stability analysis of wind turbine generator system using different drive train models," *IET Renewable Power Generation*, vol. 1, no. 2, 2007, doi: 10.1049/iet-rpg:20060030.
[17] F. Blouh, B. Boujidi, and M. Bezza, "Wind energy conversion system based on DFIG using three-phase AC-AC matrix converter," *International Journal of Power Electronics and Drive Systems (IJPEDS)*, vol. 14, no. 3, pp. 1865–1875, Sep. 2023, doi: 10.11591/ijpeds.v14.i3.pp1865-1875.
[18] M. S. Djebbar, A. Boukadoum, and A. Bouguerne, "Performances of a wind power system based on the doubly fed induction generator controlled by a multi-level inverter," *International Journal of Power Electronics and Drive Systems (IJPEDS)*, vol. 14, no. 1, pp. 100–110, Mar. 2023, doi: 10.11591/ijpeds.v14.i1.pp100-110.
[19] J. B. Ekanayake, L. Holdsworth, and N. Jenkins, "Comparison of 5th order and 3rd order machine models for doubly fed induction generator (DFIG) wind turbines," *Electric Power Systems Research*, vol. 67, no. 3, pp. 207–215, Dec. 2003, doi: 10.1016/S0378-7796(03)00109-3.
[20] D. Karnopp, "Understanding induction motor state equations using bond graphs," *Simulation Series*, vol. 35, no. 2, pp. 269–273, 2003.
[21] F. E. Cellier and E. Kofman, *Continuous system simulation*. Springer Science & Business Media, 2006.
[22] S. Junco and J. Jose, "Real-and complex-power bond graph modeling of the induction motor," *Simulation Series*, vol. 31, pp. 323–330, 1999.
[23] L. Abderrazak, R. Adlene, and K. Mohamed, "Modeling and simulation of a wind Turbine driven induction generator using bond graph," *Renewable Energy and Sustainable Development*, vol. 1, no. 2, Dec. 2015, doi: 10.21622/resd.2015.01.2.236.
[24] J. L. Domínguez-García, O. Gomis-Bellmunt, L. Trilla-Romero, and A. Junyent-Ferré, "Indirect vector control of a squirrel cage induction generator wind turbine," *Computers & Mathematics with Applications*, vol. 64, no. 2, pp. 102–114, Jul. 2012, doi: 10.1016/j.camwa.2012.01.021.
[25] B. C. GHOSH and S. N. BHADRA, "Bond graph simulation of a current source inverter driven induction motor (CSI–IM) system," *Electric Machines & Power Systems*, vol. 21, no. 1, pp. 51–67, Jan. 1993, doi: 10.1080/07313569308909634.
[26] D. Karnopp, "State functions and bond graph dynamic models for rotary, multi-winding electrical machines," *Journal of the Franklin Institute*, vol. 328, no. 1, pp. 45–54, Jan. 1991, doi: 10.1016/0016-0032(91)90005-N.
[27] D. Sahm, "A two-axis, bond graph model of the dynamics of synchronous electrical machines," *Journal of the Franklin Institute*, vol. 308, no. 3, pp. 205–218, Sep. 1979, doi: 10.1016/0016-0032(79)90113-3.
[28] B. Umesh Rai and L. Umanand, "Bond graph model of doubly fed three phase induction motor using the Axis rotator element for frame transformation," *Simulation Modelling Practice and Theory*, vol. 16, no. 10, pp. 1704–1712, Nov. 2008, doi: 10.1016/j.simpat.2008.08.012.
[29] S. Kadiman and O. Yuliani, "Model development of bond graph based wind turbine," *Indonesian Journal of Electrical Engineering and Computer Science (IJEECS)*, vol. 33, no. 2, pp. 715–726, Feb. 2024, doi: 10.11591/ijeecs.v33.i2.pp715-726.
[30] H. Dehnavifard, M. A. Khan, and P. Barendse, "Development of a 5kW scaled prototype of a 2.5 MW doubly-fed induction generator," in *2015 IEEE Energy Conversion Congress and Exposition (ECCE)*, Sep. 2015, pp. 990–996, doi: 10.1109/ECCE.2015.7309796.
[31] I. Boldea and S. A. Nasar, *The induction machines design handbook*, 2nd Edition. Boca Raton: CRC Press, 2018.
[32] R. Sanchez and A. Medina, "Wind turbine model simulation: a bond graph approach," *Simulation Modelling Practice and Theory*, vol. 41, pp. 28–45, Feb. 2014, doi: 10.1016/j.simpat.2013.11.001.

BIOGRAPHIES OF AUTHORS

Sugiarto Kadiman receives B.Eng., M.Eng., and D.Eng. in electrical engineering from DTETI, UGM, Yogyakarta, Indonesia, in 1989, 2000, and 2014, correspondingly. Since 2014, he has been conducting as associate professor in the Department of Electrical Engineering, FEP, ITNY, Yogyakarta, Indonesia. His research interests are analysis of electric power systems, simulation of dynamic structures, and electronic power control systems. The research activities comprise dynamic of synchronous generator under balanced-unbalanced conditions, advanced modelling of generator, and PSS and PID influences on transient generator. The new project is design of wind power system. He drops a line at email: sugiarto.kadiman@itny.ac.id.

Oni Yuliani holds the B.Eng. in chemical engineering from Sriwijaya University, Palembang, Indonesia, in 1996. She got M.Kom. from UGM, Yogyakarta, Indonesia in 2006. Since 1994, she has been senior lecturer in the Department of Electrical Engineering, FEP, ITNY, Yogyakarta, Indonesia. Her study attention consists of computer algorithm and stochastic processes. She could be called at email: oniyuliani@itny.ac.id.